LETTER

doi:10.1038/nature17969

Cold, clumpy accretion onto an active supermassive black hole

Grant R. Tremblay[1,2], J. B. Raymond Oonk[3,4], Françoise Combes[5], Philippe Salomé[5], Christopher P. O'Dea[6,7], Stefi A. Baum[6,8], G. Mark Voit[9], Megan Donahue[9], Brian R. McNamara[10], Timothy A. Davis[2,11], Michael A. McDonald[12], Alastair C. Edge[13], Tracy E. Clarke[14], Roberto Galván-Madrid[2,15], Malcolm N. Bremer[16], Louise O. V. Edwards[1], Andrew C. Fabian[17], Stephen Hamer[5], Yuan Li[18], Anaëlle Maury[19], Helen R. Russell[17], Alice C. Quillen[20], C. Megan Urry[1], Jeremy S. Sanders[21] & Michael W. Wise[3]

Supermassive black holes in galaxy centres can grow by the accretion of gas, liberating energy that might regulate star formation on galaxy-wide scales[1–3]. The nature of the gaseous fuel reservoirs that power black hole growth is nevertheless largely unconstrained by observations, and is instead routinely simplified as a smooth, spherical inflow of very hot gas[4]. Recent theory[5–7] and simulations[8–10] instead predict that accretion can be dominated by a stochastic, clumpy distribution of very cold molecular clouds—a departure from the 'hot mode' accretion model—although unambiguous observational support for this prediction remains elusive. Here we report observations that reveal a cold, clumpy accretion flow towards a supermassive black hole fuel reservoir in the nucleus of the Abell 2597 Brightest Cluster Galaxy (BCG), a nearby (redshift $z = 0.0821$) giant elliptical galaxy surrounded by a dense halo of hot plasma[11–13]. Under the right conditions, thermal instabilities produce a rain of cold clouds that fall towards the galaxy's centre[14], sustaining star formation amid a kiloparsec-scale molecular nebula that is found at its core[15]. The observations show that these cold clouds also fuel black hole accretion, revealing 'shadows' cast by the molecular clouds as they move inward at about 300 kilometres per second towards the active supermassive black hole, which serves as a bright backlight. Corroborating evidence from prior observations[16] of warmer atomic gas at extremely high spatial resolution[17], along with simple arguments based on geometry and probability, indicate that these clouds are within the innermost hundred parsecs of the black hole, and falling closer towards it.

We observed the Abell 2597 BCG (Fig. 1) with the Atacama Large Millimeter/submillimeter Array (ALMA), enabling us to create a three-dimensional map of both the location and motions of cold gas at uniquely high sensitivity and spatial resolution. The ALMA receivers were sensitive to emission from the $J = 2$–1 rotational line of the carbon monoxide (CO) molecule. Such CO(2–1) emission is used as a tracer of cold ($\sim$10−30 K) molecular hydrogen, which is vastly more abundant, but not directly observable at these low temperatures.

The continuum-subtracted CO(2–1) images (Fig. 2) reveal that the filamentary emission line nebula that spans the galaxy's innermost $\sim$30 kpc (Fig. 1b) consists not only of warm ionized gas[18–20], but also cold molecular gas. In projection, the optical emission line nebula is co-spatial and morphologically matched with CO(2–1) emission detected at a significance between $\gtrsim 3\sigma$ (in the outer filaments) and $\gtrsim 20\sigma$ (in the nuclear region) above the background noise level. The warm ionized nebula is therefore likely to have a substantial molecular component, consistent with results for other similar galaxies[21]. The total measured CO(2–1) line flux corresponds to a molecular hydrogen gas mass of $M_{H_2} = (1.8 \pm 0.2) \times 10^9 M_\odot$, where $M_\odot$ is the mass of the Sun. The critical (minimum) density for CO(2–1) emission requires that the volume filling factor of this gas be very low, of the order of a few per cent. The projected spatial coincidence of both the warm ionized and cold molecular nebulae therefore supports the long-envisaged hypothesis that the ionized gas is merely the warm 'skin' surrounding far colder and more massive molecular cores[22,23], whose outer regions are heated by intense radiation from the environment in which they reside. Rather than a monolithic, kiloparsec-scale slab of cold gas, we are more likely to be observing a projected superposition of many smaller, isolated clouds and filaments.

The data unambiguously show that cold molecular gas is falling inward along a line of sight that intersects the galaxy centre. We know this because the ALMA beam that is co-spatial with the millimetre continuum source, the radio core, and the isophotal centre of the galaxy reveals strong, redshifted continuum absorption (Fig. 3b), found by extracting the CO(2–1) spectrum from this central beam. This reveals at least three deep and narrow absorption lines (Fig. 3c), with redshifted line centres at +240, +275, and +335 km s^{-1} relative to the systemic (stellar) velocity of the galaxy, all within an angular (physical) region of $0.715'' \times 0.533''$ (1 kpc × 0.8 kpc).

These absorption features arise from cold molecular clouds moving towards the centre of the galaxy, via either radial or inspiralling trajectories. They manifest as continuum absorption because they cast 'shadows' along the line of sight as the clouds eclipse or attenuate about $\sim$20% (or about 2 mJy) of the millimetre synchrotron continuum source, which serves as a bright backlight (13.6 mJy at rest-frame 230 GHz). The synchrotron continuum is emitted by jets launched from the accreting supermassive ($\sim 3 \times 10^8 M_\odot$; ref. 13) black hole in the galaxy's active nucleus (Fig. 4). The absorbers must therefore be located somewhere between the observer and the galaxy centre, falling deeper into the galaxy at about +300 km s^{-1} towards the black hole at its core.

[1]Yale Center for Astronomy and Astrophysics, Yale University, 52 Hillhouse Avenue, New Haven, Connecticut 06511, USA. [2]European Southern Observatory, Karl-Schwarzschild-Strasse 2, 85748 Garching bei München, Germany. [3]ASTRON, Netherlands Institute for Radio Astronomy, PO Box 2, 7990 AA Dwingeloo, The Netherlands. [4]Leiden Observatory, Leiden University, Niels Borhweg 2, NL-2333 CA Leiden, The Netherlands. [5]Laboratory for Studies of Radiation and Matter in Astrophysics and Atmospheres (LERMA), Observatoire de Paris, PSL Research University, College de France, CNRS, Sorbonne University, Paris, France. [6]Department of Physics and Astronomy, University of Manitoba, Winnipeg, Manitoba R3T 2N2, Canada. [7]School of Physics and Astronomy, Rochester Institute of Technology, 84 Lomb Memorial Drive, Rochester, New York 14623, USA. [8]Chester F. Carlson Center for Imaging Science, Rochester Institute of Technology, 84 Lomb Memorial Drive, Rochester, New York 14623, USA. [9]Physics and Astronomy Department, Michigan State University, East Lansing, Michigan 48824-2320, USA. [10]Physics and Astronomy Department, Waterloo University, 200 University Avenue West, Waterloo, Ontario N2L 2GL, Canada. [11]School of Physics and Astronomy, Cardiff University, The Parade, Cardiff CF24 3AA, UK. [12]Kavli Institute for Astrophysics and Space Research, Massachusetts Institute of Technology, 77 Massachusetts Avenue, Cambridge, Massachusetts 02139, USA. [13]Department of Physics, Durham University, Durham DHL 3LE, UK. [14]Naval Research Laboratory Remote Sensing Division, Code 7213, 4555 Overlook Avenue Southwest, Washington DC 20375, USA. [15]Instituto de Radioastronomía y Astrofísica, UNAM, Apartado Postal 3-72 (Xangari), 58089 Morelia, Michoacán, Mexico. [16]H. W. Wills Physics Laboratory, University of Bristol, Tyndall Avenue, Bristol BS8 1TL, UK. [17]Institute of Astronomy, Cambridge University, Madingly Road, Cambridge CB3 0HA, UK. [18]Department of Astronomy, University of Michigan, 1085 South University Avenue, Ann Arbor, Michigan 48109, USA. [19]Laboratoire AIM-Paris-Saclay, CEA/DSM/Irfu CNRS—Université Paris Diderot, CE-Saclay, F-91191 Gif-sur-Yvette, France. [20]Department of Physics and Astronomy, University of Rochester, Rochester, New York 14627, USA. [21]Max-Planck-Institut für Extraterrestrische Physik, 85748 Garching bei München, Germany.

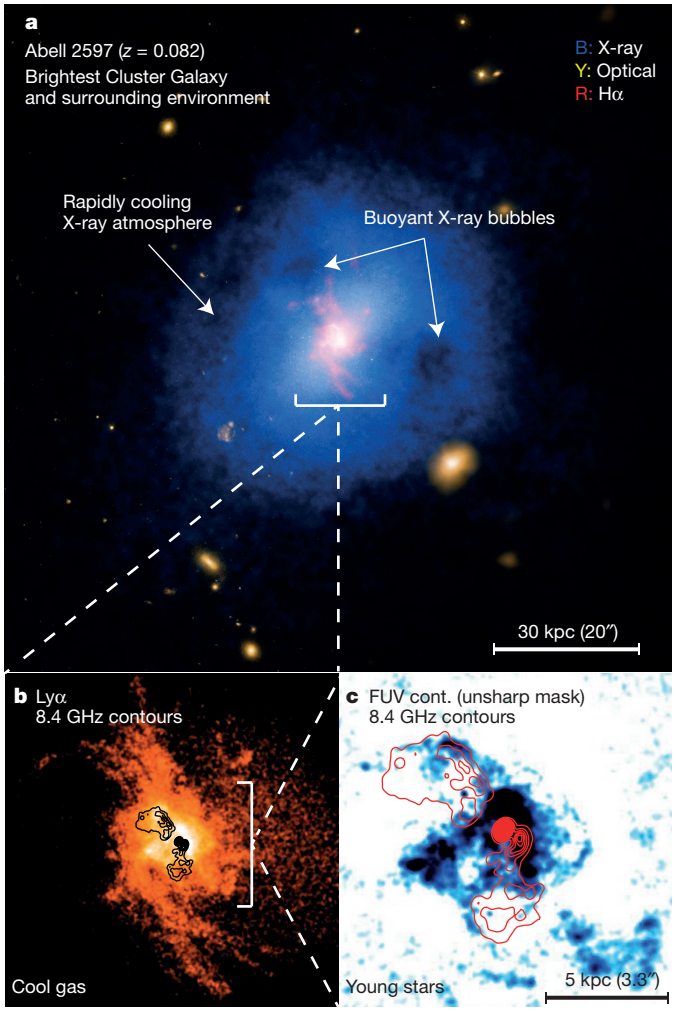

Figure 1 | A multiwavelength view of the Abell 2597 BCG. a, Chandra X-ray, HST and DSS optical, and Magellan Hα+[N II] emission is shown in blue, yellow and red, respectively. Arrows point to the thermally unstable hot atmosphere and buoyant bubbles that permeate it. (Image credits: X-ray, NASA/CXC/Michigan State University/G. Voit *et al.*; optical, NASA/STScI and DSS; Hα, Carnegie Observatory/Magellan/W. Baade Telescope/University of Maryland/M. McDonald). **b**, HST image of Lyα emission associated with the ionized gas nebula[13], with 8.4 GHz radio contours overlaid in black. The filamentary ionized nebula consists of cooler gas that has precipitated from the hot X-ray bright halo shown in **a**. **c**, Unsharp mask of the HST far-ultraviolet (FUV) continuum image of the central regions of the nebula[15]. The FUV emission directly traces the locations of young stars in the nebula. Very Large Array (VLA) radio contours of the 8.4 GHz source are overlaid in red.

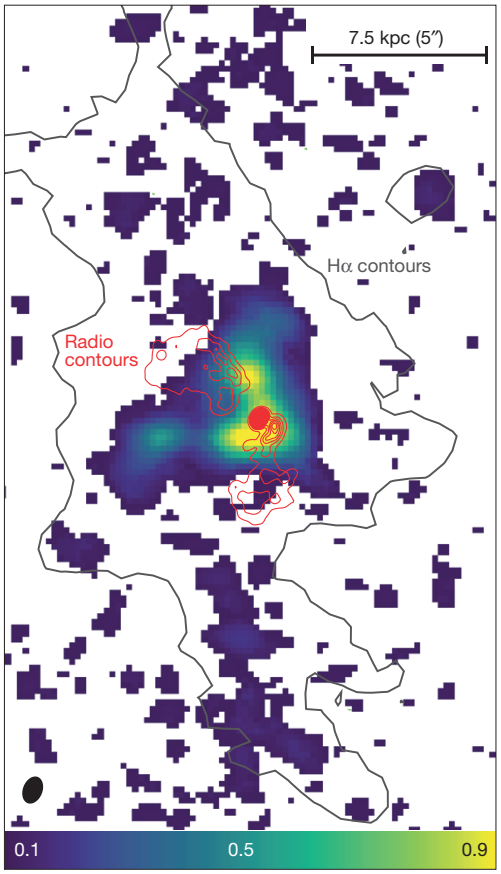

Figure 2 | ALMA observation of continuum-subtracted CO(2–1) emission in the Abell 2597 BCG. Emission is integrated from $-600\,\mathrm{km\,s^{-1}}$ to $+600\,\mathrm{km\,s^{-1}}$ relative to the galaxy's systemic velocity. Channels are binned to $40\,\mathrm{km\,s^{-1}}$. Only $\geq 3\sigma$ emission is shown. 8.4 GHz VLA radio contours are overlaid in black, and Hα contours outlining the rough boundary of the ionized nebula are shown in grey. The nebula is slightly larger than the grey contours suggest: emission outside this boundary is still part of a smooth, fainter distribution of cold gas, co-spatial with similarly faint emission in the optical.

This radial speed is roughly equal to the expected circular velocity[24] in the nucleus, consistent either with a nearly radial orbit, or with highly non-circular motions in close proximity to the galaxy's core.

Gaussian fits to the spectral absorption features reveal narrow linewidths of $\sigma_v \lesssim 6\,\mathrm{km\,s^{-1}}$, which means the absorbers are more probably spatially compact, with sizes that span tens (rather than hundreds or thousands) of parsecs. The shapes of the absorption lines remain roughly the same regardless of how finely the spectra are binned, suggesting that the absorbers are probably coherent structures, rather than a superposition of many smaller absorbers unresolved in velocity space. If each absorption feature corresponds to one coherent cloud, and if those clouds roughly obey size–linewidth relations[25,26] for giant molecular clouds in the Milky Way, they should have diameters not larger than ~40 pc. If in virial equilibrium, molecular clouds this size would have masses of the order of 10^5–$10^6\,M_\odot$, and if in rough pressure equilibrium with their ambient multiphase (10^3–10^7 K) environment[13], they must have high column densities of the order of $N_{H_2} \approx 10^{22} - 10^{24}\,\mathrm{cm^{-2}}$ so as to maintain pressure support. The thermal pressure in the core of Abell 2597 BCG is nearly 3,000 times[13] greater than that for the Milky Way, however, which means the absorbing clouds may be much smaller.

The absorbers have optical depths in the range $0.1 \lesssim \tau_{CO(2-1)} \lesssim 0.3$. The physical resolution of the ALMA data is larger than the synchrotron background source, which means that the optical depth is probably contaminated by an unresolved, additive superposition of both emission and absorption within the beam. Compact, dense cold clouds are nevertheless likely to be optically thick, which may mean they eclipse the continuum source with an optical depth of unity but a small covering factor of roughly 0.2. Especially when considering beam contamination by emission, the covering factor cannot be known with certainty, as this depends on the unknown geometry of the absorbing and emitting regions within the ALMA beam.

This geometry can be constrained, however, given existing Very Long Baseline Array (VLBA) radio observations at extremely high spatial resolution[17]. These data resolve the 1.3 GHz and 5 GHz radio continuum source down to scales of 25 pc, revealing a highly symmetric, 100-pc-scale jet about a bright radio core (Fig. 4c). Just as we have found in cold molecular gas, inflowing warmer atomic hydrogen gas (H I) has previously been found in absorption against this parsec-scale jet, corroborating prior reports of inflowing atomic gas at lower spatial resolutions[16]. The inflow velocity of this gas matches that seen

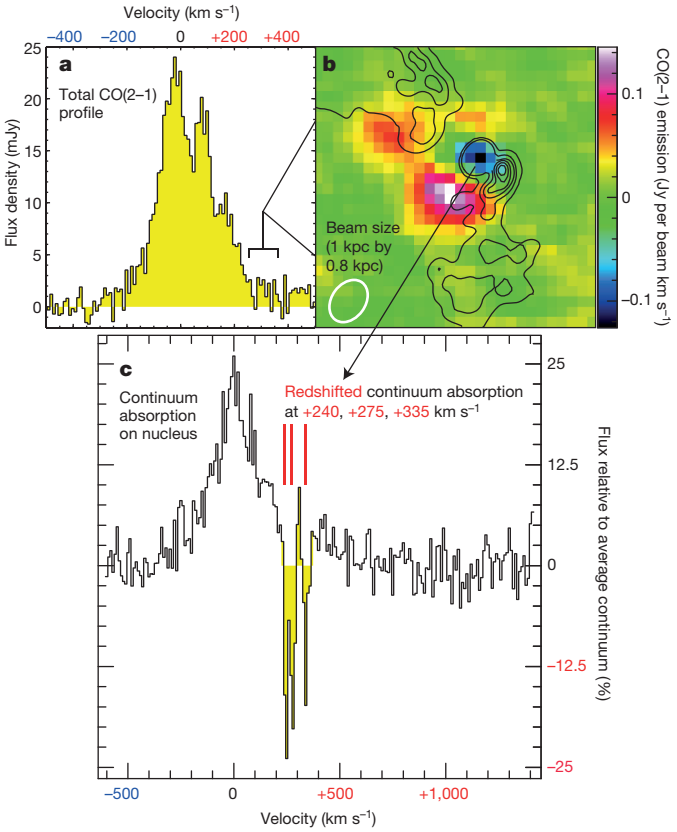

Figure 3 | 'Shadows' cast by molecular clouds moving towards the supermassive black hole. a, Continuum-subtracted ALMA CO(2–1) spectrum extracted from a central 10 kpc region. Brackets mark CO(2–1) emission shown in **b**, where 8.4 GHz radio contours are overlaid. The central radio contours have been removed to aid viewing of the continuum absorption, seen as the blue/black spot of 'negative' emission (which is the radio and mm core, the centre of the galaxy and the location of the black hole). **c**, Continuum-subtracted CO(2–1) spectrum extracted from this region co-spatial with the mm and radio core. Absorption lines are indicated in red.

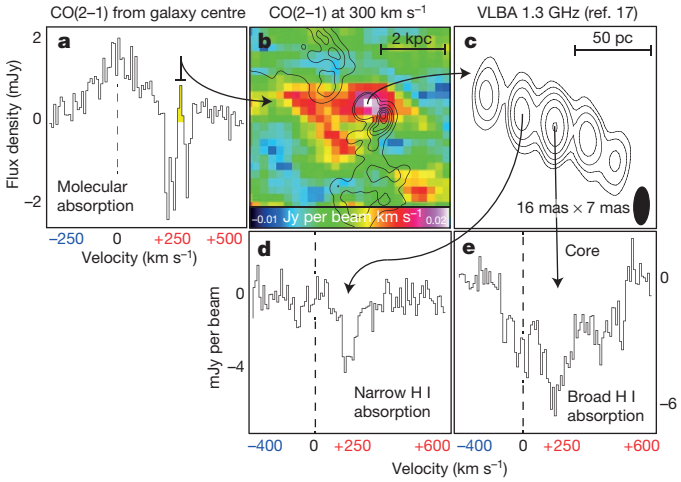

Figure 4 | Corroborating evidence that the inflowing molecular clouds must be in close proximity to the black hole. a, CO(2–1) absorption spectrum from Fig. 3, with a region of emission at about +300 km s^{-1} marked in yellow. **b**, Integrated CO(2–1) emission (colour coded) from this region, showing that gas at about +300 km s^{-1} is confined to the innermost 2 kpc of the galaxy. **c**, 1.3 GHz radio continuum source from an archival VLBA observation[17] with an extremely high physical resolution of ~25 pc by ~10 pc. **d**, **e**, Plots of 1.3 GHz radio continuum emission revealing H I 21 cm absorption observed against this synchrotron jet. The signal varies dramatically over scales of tens of parsecs.

in our ALMA data. Remarkably, both the optical depth and linewidth of the warm atomic absorption signal varies dramatically across the jet, with a broad ($\sigma_v \approx 310$ km s^{-1}) component co-spatial with the core that is absent just ~20 pc to the northeast, where only a narrow ($\sigma_v \approx 50$ km s^{-1}) H I line is found at the same redshift. This effectively requires the inflowing atomic gas to be confined within the innermost ~100 pc of the black hole, as gas further out would give rise to an unchanging absorption signal across the compact jet. The infall velocity is the same as that for the cold molecular clouds seen in CO(2–1) absorption, which means they most probably stem from the same spatial region, within tens of parsecs of the accreting black hole.

This is further supported by the ALMA data itself. In emission, all gas around approximately +300 km s^{-1} that is conceivably available to attenuate the continuum signal is confined to the innermost 2 kpc about the nucleus (Fig. 4a, b). The radial dependence of molecular cloud volume number density within this region is uncertain, but probably steeper than r^{-1}, and likely to be closer to r^{-2} (Fig. 4b). This means that the chances of a random line of sight crossing will drop with increasing distance from the black hole. If the gas volume density goes as r^{-2}, a cloud 100 pc from the black hole is ten times more likely to cross our line of sight than a cloud at a galactocentric distance of 1 kpc. It would be exceedingly unlikely for three such clouds to cross our line of sight to the black hole were they spread over several kiloparsecs throughout the galaxy's outskirts.

The data therefore serve as strong observational evidence for an inward-moving, clumpy distribution of molecular clouds within a few hundred parsecs of an accreting supermassive black hole. The result augments a small but growing set of known molecular absorption systems[27–29] whose black hole proximity is less well constrained. The infalling clouds in Abell 2597 BCG are probably a few to tens of parsecs across and therefore massive (perhaps 10^5–10^6 $M_\odot$ each). If they are falling directly towards the black hole, rather than bound in a non-circular orbit that tightly winds around it, they could supply an upper-limit accretion rate of the order of ~0.1 to a few solar masses per year, depending on the three-dimensional distribution of infalling clouds. If most of the clouds are instead locked in non-circular orbits around the black hole, the fuelling rate would depend on the gas angular momentum, and the local supply of torques that might lessen it. Simulations suggest[9,10,14] that such torques may be plentiful, as they predict a stochastic 'rain' of thermal instabilities that condense from all directions around the black hole, promoting angular momentum cancellation via tidal stress and cloud–cloud collisions. Even highly elliptical cloud orbits should therefore be associated with significant inward radial motions. The clouds might fall onto the accretion disk itself, or into a clumpy rotating ring akin to the 'torus' invoked in AGN unification models[30].

Online Content Methods, along with any additional Extended Data display items and Source Data, are available in the online version of the paper; references unique to these sections appear only in the online paper.

Received 17 December 2015; accepted 22 March 2016.

1. McNamara, B. R. & Nulsen, P. E. J. Heating hot atmospheres with active galactic nuclei. *Annu. Rev. Astron. Astrophys.* **45,** 117–175 (2007).
2. McNamara, B. R. & Nulsen, P. E. J. Mechanical feedback from active galactic nuclei in galaxies, groups and clusters. *New J. Phys.* **14,** 055023 (2012).
3. Fabian, A. C. Observational evidence of active galactic nuclei feedback. *Annu. Rev. Astron. Astrophys.* **50,** 455–489 (2012).
4. Bondi, H. On spherically symmetrical accretion. *Mon. Not. R. Astron. Soc.* **112,** 195–204 (1952).
5. Pizzolato, F. & Soker, N. On the nature of feedback heating in cooling flow clusters. *Astrophys. J.* **632,** 821–830 (2005).
6. Voit, G. M., Donahue, M., Bryan, G. L. & McDonald, M. Regulation of star formation in giant galaxies by precipitation, feedback and conduction. *Nature* **519,** 203–206 (2015).
7. Voit, G. M., Bryan, G. L., O'Shea, B. W. & Donahue, M. Precipitation-regulated star formation in galaxies. *Astrophys. J.* **808,** L30 (2015).

8. Sharma, P., McCourt, M., Quataert, E. & Parrish, I. J. Thermal instability and the feedback regulation of hot haloes in clusters, groups, and galaxies. *Mon. Not. R. Astron. Soc.* **420,** 3174–3194 (2012).
9. Gaspari, M., Ruszkowski, M. & Oh, S. P. Chaotic cold accretion on to black holes. *Mon. Not. R. Astron. Soc.* **432,** 3401–3422 (2013).
10. Li, Y. & Bryan, G. L. Modeling active galactic nucleus feedback in cool-core clusters: the formation of cold clumps. *Astrophys. J.* **789,** 153 (2014).
11. McNamara, B. R. *et al.* Discovery of ghost cavities in the X-ray atmosphere of Abell 2597. *Astrophys. J.* **562,** L149–L152 (2001).
12. Clarke, T. E., Sarazin, C. L., Blanton, E. L., Neumann, D. M. & Kassim, N. E. Low-frequency radio observations of X-ray ghost bubbles in A2597: a history of radio activity in the core. *Astrophys. J.* **625,** 748–753 (2005).
13. Tremblay, G. R. *et al.* Multiphase signatures of active galactic nucleus feedback in Abell 2597. *Mon. Not. R. Astron. Soc.* **424,** 1026–1041 (2012).
14. Gaspari, M., Brighenti, F. & Temi, P. Chaotic cold accretion on to black holes in rotating atmospheres. *Astron. Astrophys.* **579,** A62 (2015).
15. Tremblay, G. R. *et al.* Residual cooling and persistent star formation amid active galactic nucleus feedback in Abell 2597. *Mon. Not. R. Astron. Soc.* **424,** 1042–1060 (2012).
16. O'Dea, C. P., Baum, S. A. & Gallimore, J. F. Detection of extended H I absorption toward PKS 2322–123 in Abell 2597. *Astrophys. J.* **436,** 669–677 (1994).
17. Taylor, G. B., O'Dea, C. P., Peck, A. B. & Koekemoer, A. M. H I Absorption toward the nucleus of the radio galaxy PKS 2322–123 in A2597. *Astrophys. J.* **512,** L27–L30 (1999).
18. O'Dea, C. P., Baum, S. A., Mack, J., Koekemoer, A. M. & Laor, A. Hubble Space Telescope STIS far-ultraviolet observations of the central nebulae in the cooling-core clusters A1795 and A2597. *Astrophys. J.* **612,** 131–151 (2004).
19. Oonk, J. B. R., Hatch, N. A., Jaffe, W., Bremer, M. N. & van Weeren, R. J. Far-ultraviolet emission in the A2597 and A2204 brightest cluster galaxies. *Mon. Not. R. Astron. Soc.* **414,** 2309–2336 (2011).
20. Tremblay, G. R. *et al.* Far-ultraviolet morphology of star-forming filaments in cool core brightest cluster galaxies. *Mon. Not. R. Astron. Soc.* **451,** 3768–3800 (2015).
21. Salomé, P. *et al.* A very extended molecular web around NGC 1275. *Astron. Astrophys.* **531,** A85 (2011).
22. Jaffe, W., Bremer, M. N. & Baker, K. H II and H_2 in the envelopes of cooling flow central galaxies. *Mon. Not. R. Astron. Soc.* **360,** 748–762 (2005).
23. Salomé, P. *et al.* Cold molecular gas in the Perseus cluster core. Association with X-ray cavity, Hα filaments and cooling flow. *Astron. Astrophys.* **454,** 437–445 (2006).
24. Smith, E. P., Heckman, T. M. & Illingworth, G. D. Stellar dynamics of powerful radio galaxies. *Astrophys. J.* **356,** 399–415 (1990).
25. Larson, R. B. Turbulence and star formation in molecular clouds. *Mon. Not. R. Astron. Soc.* **194,** 809–826 (1981).
26. Solomon, P. M., Rivolo, A. R., Barrett, J. & Yahil, A. Mass, luminosity, and line width relations of Galactic molecular clouds. *Astrophys. J.* **319,** 730–741 (1987).
27. Wiklind, T. & Combes, F. Molecular absorption and its time variations in Centaurus A. *Astron. Astrophys.* **324,** 51–64 (1997).
28. Espada, D. *et al.* Disentangling the circumnuclear environs of Centaurus A. II. On the nature of the broad absorption line. *Astrophys. J.* **720,** 666–678 (2010).
29. David, L. P. *et al.* Molecular gas in the X-ray bright group NGC 5044 as revealed by ALMA. *Astrophys. J.* **792,** 94 (2014).
30. Urry, C. M. & Padovani, P. Unified schemes for radio-loud active galactic nuclei. *Publ. Astron. Soc. Pacif.* **107,** 803–845 (1995).

Acknowledgements ALMA is a partnership of ESO (representing its member states), NSF (USA) and NINS (Japan), together with NRC (Canada) and NSC and ASIAA (Taiwan), in cooperation with the Republic of Chile. The Joint ALMA Observatory is operated by ESO, AUI/NRAO and NAOJ. We are grateful to the European ALMA Regional Centres, particularly those in Garching and Manchester, for their dedicated end-to-end support of data associated with this paper. We thank R. Larson for discussions. G.R.T. acknowledges support from National Aeronautics and Space Administration (NASA) through Einstein Postdoctoral Fellowship Award Number PF-150128, issued by the Chandra X-ray Observatory Center, which is operated by the Smithsonian Astrophysical Observatory for and on behalf of NASA under contract NAS8-03060. F.C. acknowledges the European Research Council (ERC) for the Advanced Grant Program no. 267399-Momentum. B.R.M. is supported by a grant from the Natural Sciences and Engineering Research Council of Canada. T.A.D. acknowledges support from a Science and Technology Facilities Council (STFC) Ernest Rutherford Fellowship. A.C.E. acknowledges support from STFC grant ST/L00075X/1. A.C.F. and H.R.R. acknowledge support from ERC Advanced Grant Program no. 340442-Feedback. M.N.B. acknowledges funding from the STFC. Basic research in radio astronomy at the Naval Research Laboratory is supported by 6.1 Base funding.

Author Contributions G.R.T. was principal investigator on the original proposal, performed the data analysis, and wrote the paper. J.B.R.O., T.A.D., R.G.M. and A.M. were substantially involved in planning both scientific and technical aspects of the proposal, while T.A.D. and R.G.M. contributed ALMA data reduction and analysis expertise once the data were obtained. J.B.R.O., F.C. and P.S. invested substantial time in analysis of the data. Substantial scientific feedback was also provided over many months by F.C., J.B.R.O., C.P.O., S.A.B., G.M.V., M.D., B.R.M., M.A.M., T.E.C., H.R., A.C.E. and A.C.F., while all other co-authors discussed the results and commented on the manuscript.

Author Information This paper makes use of the following ALMA data: ADS/JAO.ALMA#2012.1.00988.S. Reprints and permissions information is available at www.nature.com/reprints. The authors declare no competing financial interests. Readers are welcome to comment on the online version of the paper. Correspondence and requests for materials should be addressed to G.R.T. (grant.tremblay@yale.edu).

METHODS

Observations, data reduction, and analysis. The new ALMA data presented in this paper were obtained in Cycle 1 with the use of 29 operational antennae in the 12 m Array. ALMA's Band 6 heterodyne receivers were tuned to a frequency of 213 GHz, sensitive to the $J=2$–1 rotational line transition of carbon monoxide at the redshift of the Abell 2597 BCG ($z=0.0821$). The ALMA correlator, set to Frequency Division Mode (FDM), delivered a bandwidth of 1,875 MHz (per baseband) with a 0.488 MHz channel spacing, for a maximum spectral resolution of about 2 km s^{-1}. One baseband was centred on the CO(2–1) emission line, while the other three sampled the local continuum. Maximum antenna baselines extended to ~1 km, delivering an angular resolution at 213 GHz of ~0.7″ within a ~28″ primary beam (field of view). ALMA observed the Abell 2597 BCG, located at RA 23 h 25 min 20 s, dec. −12° 07′ 38″ (J2000), for a total of ~3 h over three separate scheduling blocks executed between 17 and 19 November 2013. The planet Neptune and quasars J2258−2758 and J2331−1556 were used for amplitude, flux, and phase calibration. The data were reduced using CASA version 4.2 with calibration and imaging scripts kindly provided by the ALMA Regional Centers (ARCs) in both Garching, Germany and Manchester, UK. Beyond the standard application of the phase calibrator solution, we iteratively performed self-calibration of the data using the galaxy's own continuum, yielding a ~14% decrease in RMS noise to a final value of 0.16 mJy per 0.715″ × 0.533″ beam per 40 km s^{-1} channel. There is effectively no difference in CO(2–1) morphology between the self-calibrated and non-self-calibrated data cubes. Measurement sets were imaged using 'natural' visibility weighting and binning to either 5 km s^{-1}, 10 km s^{-1}, or 40 km s^{-1}, as indicated in the figure legends. The figures presented in this Letter show only continuum-subtracted, pure CO(2–1) line emission. The rest-frame 230 GHz continuum observation is dominated by a bright (13.6 mJy) point source associated with the AGN (detected at $\gtrsim 400\sigma$), serving as the bright 'backlight' against which the continuum absorption features presented in this Letter were observed. The continuum data also features compact (~5 kpc) extended emission at ~10σ that extends along the galaxy's dust lane, to be discussed in a forthcoming paper.

Adoption of a systemic velocity. Interpretation of gas motions relative to the stellar component of a galaxy requires adoption of a systemic (stellar) velocity to be used as a 'zero point' marking the transition from blue- to redshift. All CO(2–1) line velocities discussed in this Letter are set relative to 213.04685 GHz, where observed CO(2–1) emission peaks. This frequency corresponds to ^{12}CO(2–1) (rest-frame 230.538001 GHz) at a redshift of $z=0.0821$. This redshift is consistent, conservatively within ±60 km s^{-1}, with every other available multiwavelength tracer of the galaxy's systemic velocity, including prominent Ca II H, K, and G-band absorption features[17] that directly trace the galaxy stellar component, the redshift of all optical emission lines[31], as well as a broad (FWHM 412 km s^{-1}) H I absorption component[16] at the optical emission and absorption line redshift. It is also consistent, within ~60 km s^{-1}, with a cross-correlation of emission and absorption lines using galaxy template spectra[17], as well as with all other published reports of the galaxy's systemic velocity (found, for example, within the HyperLeda database). We are therefore certain that the reported redshift of the absorption features discussed in this Letter indeed corresponds to real motion relative to the galaxy's stellar component. Without caveat or ambiguity, the absorbing cold clouds are moving into the galaxy at roughly ~300 ± 60 km s^{-1}.

Mass estimates. All molecular gas masses estimated in this letter adopt the following relation[32]:

$$M_{\rm mol}=\frac{1.05\times10^4}{3.2}\left(\frac{X_{\rm CO}}{2\times10^{20}\frac{\rm cm^{-2}}{\rm K\ km\ s^{-1}}}\right)\left(\frac{1}{1+z}\right)\left(\frac{S_{\rm CO}\Delta v}{\rm Jy\ km\ s^{-1}}\right)\left(\frac{D_{\rm L}}{\rm Mpc}\right)^2 M_\odot$$

where $S_{\rm CO}\Delta v$ is the emission integral (effectively the total CO flux over the region of interest), z is the galaxy redshift ($z=0.0821$), and $D_{\rm L}$ its luminosity distance (373.3 Mpc), for which we assume a flat ΛCDM model wherein $H_0=70$ km s^{-1} Mpc^{-1}, $\Omega_{\rm M}=0.3$, and $\Omega_\Lambda=0.7$. This mass estimate most critically relies on an assumption of the CO-to-H_2 conversion factor[32], $X_{\rm CO}$. In this Letter we assume the average Milky Way value of $X_{\rm CO}=2\times10^{20}$ cm^{-2} (K km s^{-1})$^{-1}$ and a CO(2–1) to CO(1–0) flux density ratio of 3.2. Other authors have provided extensive discussion of these assumptions as they pertain to cool core BCGs[29,33,34]. Scientific conclusions in this paper are largely insensitive to choice of $X_{\rm CO}$.

A single Gaussian fit to the CO(2–1) spectrum extracted from an aperture containing all detected emission yields an emission integral of $S_{\rm CO}\Delta v=4.2\pm0.4$ Jy km s^{-1} with a line FWHM of 252 ± 14 km s^{-1}, corresponding to a total molecular hydrogen (H_2) gas mass of $M_{\rm H_2}=(1.80\pm0.19)\times10^9\ M_\odot$. This is very close to the previously reported[15] mass, based on an IRAM 30m CO(2–1) observation, of $(1.8\pm0.3)\times10^9\ M_\odot$. This comparison is not one-to-one, as the mass from the IRAM 30m observation was computed from within a beam size of 11″ (rather than 28″ for the ALMA data), and used a CO(2–1)/CO(1–0) flux ratio of 4 (rather than 3.2, as we use here). These differences are minor, particularly because nearly all of the CO(2–1) emission detected by ALMA is found within the central 11″ size of the IRAM 30m beam. It is therefore safe to say that our ALMA observation has detected nearly all emission that was detected in the single-dish IRAM 30m observation, and that very little extended emission has been 'resolved out' by ALMA.

Estimating physical properties of the redshifted absorbing molecular gas. We have estimated a rough upper-limit size of the absorbing clouds assuming the widely adopted Larson *et al.*[25] and Solomon *et al.*[26] size–linewidth relation for molecular clouds in the Milky Way (namely, the ref. 26 fit);

$$\sigma_v=(1.0\pm0.1)S^{0.5\pm0.05}\ {\rm km\ s^{-1}}$$

where σ_v is the velocity linewidth of the cloud and S is the diameter of the cloud in parsecs. A measured absorber linewidth of $\sigma_v\approx6$ km s^{-1} would then correspond to a size of ~36 pc. As noted in the main text of the Letter, the thermal pressure in the Abell 2597 BCG is about 3,000 times higher than that for the Milky Way[13], so it is likely that the above relation does not apply. A higher ambient pressure implies higher compression and therefore smaller cloud size, so the above estimate should, at best, be considered a very rough upper-limit. The main lesson to take away from this exercise is that the absorbing clouds are probably physically compact (that is, a few to tens—rather than hundreds—of parsecs in diameter).

The three clouds are separated from one another by ~45–60 km s^{-1} in velocity space, which means they are unlikely to be closely bound satellites of one another. Instead, it is more likely that they represent three random points along a radial distribution of clouds.

If the absorbers are in virial equilibrium, their masses $M_{\rm cloud}$ can be roughly estimated by applying the virial relation,

$$M_{\rm cloud}\approx\frac{R_{\rm cloud}\sigma_v^2}{G}\approx\frac{20{\rm pc}\times(6\ {\rm km\ s^{-1}})^2}{4.302\times10^{-3}\ {\rm pc}\ M_\odot^{-1}({\rm km\ s^{-1}})^2}\approx1.7\times10^5\ M_\odot$$

where $R_{\rm cloud}$ is the cloud radius (as roughly estimated above) and σ_v is its velocity dispersion (also as above).

CO(2–1) optical depths for the absorbers were estimated by assuming that:

$$I_{\rm total}=I_{\rm continuum}e^{-\tau_{\rm CO(2-1)}}$$

where $I_{\rm total}$ and $I_{\rm continuum}$ are the integrated intensities of the total (line plus continuum) and continuum-only signals, respectively, and $\tau_{\rm CO(2-1)}$ is the optical depth of the CO(2–1) absorption feature.

The stellar velocity dispersion of the BCG[33] is $\sigma_v=220\pm19$ km s^{-1}. Under the assumption of an isothermal sphere, the circular velocity should be ~300 km s^{-1} (that is, $\sqrt{2}\,\sigma_v$), which is roughly the line of sight velocity of the absorption features. That the absorbers' redshift is a significant fraction of the expected circular velocity means they could be on a nearly radial orbit (though their transverse velocity cannot be known with this single observation).

While not discussed in the main text, there is an additional simple argument that independently suggests that the inward moving molecular clouds must be in close proximity to the black hole. If our line of sight is representative, and therefore a 'pencil beam' sample of a three-dimensional spherical distribution of clouds, the total mass of cold gas contained within this distribution should go roughly as:

$$M\approx10^9M_\odot\times f_{\rm c}\times\left(\frac{r}{1\ {\rm kpc}}\right)^2\times\left(\frac{N_{\rm H}}{10^{22}{\rm cm^{-2}}}\right)$$

where $f_{\rm c}$ is the covering factor and r is the radius of an imaginary thin spherical shell of molecular gas with column density $N_{\rm H}$. If such a shell had a covering factor of 1, a radius of 1 kpc, and a column density of 10^{22} cm^{-2}, then the total mass of molecular hydrogen contained within that shell would be roughly one billion solar masses. A column density in excess of 10^{22} cm^{-2} requires this distribution to be contained within a sphere of radius $<<1$ kpc, lest the limit set by the total mass of molecular hydrogen in the galaxy be violated. If the characteristic column density is 10^{23} cm^{-2}, for example, this mass must be contained within a sphere of radius 300 pc, or else its total mass would exceed the $1.8\times10^9\ M_\odot$ of cold gas present in the galaxy.

Codes, software, and data availability. Codes that we have written to both reduce and analyse the data presented in this Letter have been made publicly available at https://github.com/granttremblay/Tremblay_Nature_ALMA_Abell2597. Reduction of the data as well as some simple modelling (for example, fitting of Gaussians to lines) was performed using routines included in CASA version 4.2, available at https://casa.nrao.edu/. Plots were made using both Python's MatPlotLib and *Veusz*, which is available at http://home.gna.org/veusz/.

31. Voit, G. M. & Donahue, M. A deep look at the emission-line nebula in Abell 2597. *Astrophys. J.* **486,** 242 (1997).
32. Bolatto, A. D., Wolfire, M. & Leroy, A. K. The CO-to-H_2 conversion factor. *Annu. Rev. Astron. Astrophys.* **51,** 207–268 (2013).
33. McNamara, B. R. *et al.* A 10^{10} solar mass flow of molecular gas in the A1835 brightest cluster galaxy. *Astrophys. J.* **785,** 44 (2014).
34. Russell, H. R. *et al.* Massive molecular gas flows in the A1664 brightest cluster galaxy. *Astrophys. J.* **784,** 78 (2014).